Correlation between hole density and oxygen excess in the $Bi_2Sr_2CaCu_2O_{8+\delta}$ superconductor

P. Ghigna, G. Spinolo, G. Flor, and N. Morgante
INCM, C.S.T.E./CNR, Dipartimento di Chimica Fisica, Università di Pavia, V.le Taramelli 16, I-27100 Pavia, Italy
(Received 9 January 1998)

Charge-carrier density in Bi-2212 oxide superconductor samples with well-defined cation molecularity has been measured by means of Cu-L_{III} x-ray absorption spectroscopy, as a function of the oxygen content, which was fixed to known values by annealing at predetermined T and $P(O_2)$, and subsequent quenching. The main results of this work can be summarized as follows: (i) at low oxygen content the hole density is greater than that one determined by the oxygen excess only; (ii) at intermediary oxygen content values the hole density is almost entirely determined by the oxygen excess only; each extra oxygen atom contributes two holes to the overall charge-carrier density; (iii) for the highest values of the oxygen content, each extra oxygen atom contributes only one hole to the overall charge-carrier density. From these results a band model is drawn in which the extra oxygen levels lie in energy near the Fermi level. [S0163-1829(98)04022-3]

The oxide superconductor usually known as BSCCO-2212 or Bi-2212 (i.e., with $Bi_2Sr_2CaCu_2O_{8+\delta}$ reference composition) has been deeply investigated in the last years with x-ray-absorption spectroscopy (XAS) to gain insight into its electronic structure[1–14] in the normal and superconducting states, and into the modifications produced by injecting holes with different mechanisms of doping. Many fine details of its complicated electronic structure have been elucidated with a number of careful experiments on the Bi-L_{III}, Cu-K, and (mostly) O-K and Cu-L_{III} edges, also using polarized x-ray-absorption and high-quality single crystals. There is now general agreement on the nature of the itinerant states having a predominant oxygen $2p$ character mixed with a copper $3d$ character, i.e., doping induces holes in a band having a predominant Cu-O antibonding character. It is also well known that a significant overlap with another antibonding band pertinent to the [BiO] layers produces a charge transfer, which can be seen as a partial oxidation of the $[CuO_2]$ planes by the [BiO] planes. It has also been shown that, likely due to local structural relaxation in the $[CuO_2]$ planes, there is a significant increase in the relative amount of itinerant holes below T_c.[11,12]

These features, the related properties of the phase, and the onset of superconductivity, dramatically depend on the amount and kind of doping. It is important to note that the oxidizing effect of the [BiO] planes causes the relationship between the hole density and the oxygen content to be nonlinear. It is therefore worthwhile to investigate how the electronic structure of BSCCO-2212 is modified when varying the independent thermodynamic variables corresponding to the amount of additional oxygens on normally empty sites. To this purpose, we have prepared a series of BSCCO samples with well-defined cationic composition and with different amounts of oxygen nonstoichiometry. A synthetic pathway based on a solid-state reaction along a pseudobinary cut of the overall Bi, Sr, Ca, Cu/O system has been used to achieve a precise molecularity. With this method, a couple of suitably selected single-phase materials is allowed to react in such a way that only one product phase can form. Then, different batches of the BSCCO phase have been submitted to different thermal cycles under different oxygen partial pressures to unambiguously fix the oxygen content, and quenched. After determination of molecularity and oxygen stoichiometry, the samples have been investigated by Cu-L_{III} edge XAS.

The BSCCO (2212) materials were prepared by solid-state reaction, starting from $Sr_{14}Cu_{24}O_{41}$ and $Ca_{0.376}Sr_{0.082}Bi_{0.543}O_{1.273}$.[15] This corresponds to a pseudobinary cut in the Ca, Sr, Cu, Bi/O pseudoquaternary phase diagram, so that only the desired product is allowed to form during the reaction. $Sr_{14}Cu_{24}O_{41}$ was prepared starting from CuO (Aldrich, 99.99%) and $SrCO_3$ (Atomergic Chemetals 99.999%). The starting materials were weighted in the proper stoichiometric ratio, mixed in acetone and stirred overnight. The homogeneous mixture obtained after acetone evaporation was pressed into pellets and heated at 800 °C under pure oxygen flow for more than 100 h, with two intermediate grinding and repressing steps. $Ca_{0.376}Sr_{0.082}Bi_{0.543}O_{1.273}$ was prepared with a similar procedure starting from Bi_2O_3 (Aldrich, 99.99%), $CaCO_3$ (Atomergic Chemetals 99.999%), and $SrCO_3$ (Atomergic Chemetals 99.999%). The homogeneous mixture obtained after acetone evaporation was pressed into pellets and heated at 800 °C under pure oxygen flow for more than 72 h, with two intermediate grinding and repressing steps. The reaction between the two parent materials to give the desired BISCCO (2212) phase was achieved at 750 °C under a flow of an N_2/O_2 mixture with $P(O_2)=10^{-3}$ atm, for more than 450 h, with six intermediate grinding and re-pressing steps. Samples with different oxygen contents have been prepared by annealing the as-prepared material at appropriate T and $P(O_2)$.

The determination of the oxygen nonstoichiometry was carried out in a homemade apparatus built starting from a Cahn 2000 thermobalance, in flowing pure oxygen, in the range $25 \leqslant T\ (°C) \leqslant 750$. For the measurements, $\cong 120$ mg of the BISCCO material were preliminarily annealed at 800 °C in flowing pure oxygen for 50 h, and then cooled down to room temperature at a rate of 1 °C/min. The sample was then introduced in the thermobalance and submitted to a thermal cycle consisting of a ramp by 1 °C/min and isothermal steps of 16 h after every 50 °C. The thermal cycle was accom-

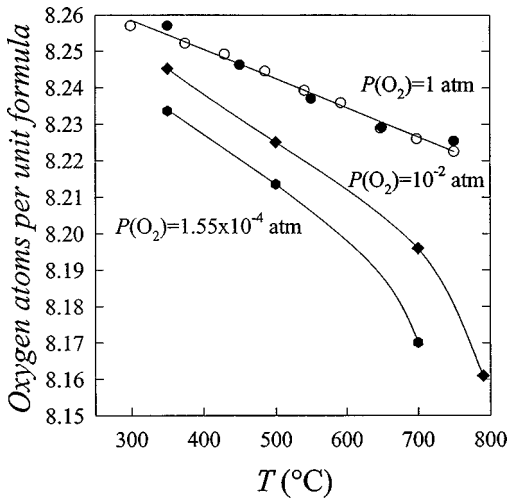

FIG. 1. Oxygen nonstoichiometry in $Bi_{2.15}Sr_{1.48}Ca_{1.37}Cu_2O_{8.075+\delta}$, under different T and $P(O_2)$. Circles, diamonds, and hexagons refer to $P(O_2)=1$, 10^{-2}, and 1.55×10^{-4} atm, respectively. For the 1 atm plot, hollow and filled symbols refer to two different sets of measures. Lines in this figure are eye guidelines.

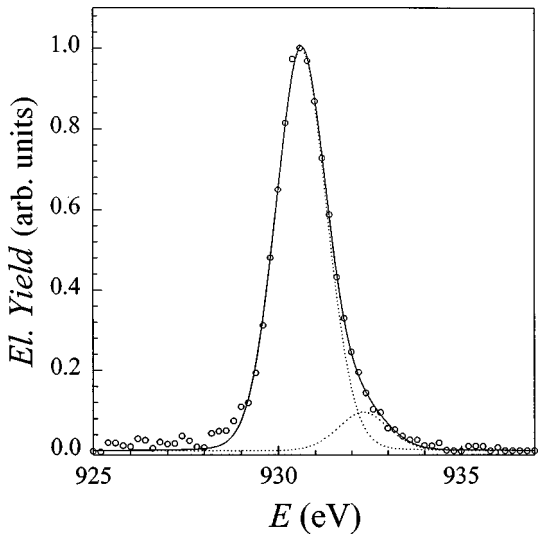

FIG. 2. Cu-L_{III} spectrum of a $Bi_{2.15}Sr_{1.48}Ca_{1.37}Cu_2O_{8.145}$ sample, after background subtraction. Dots are the experimental data, while dashed and full lines refer to partial and total fit with pseudo-Voigt functions.

plished both in heating and in cooling; full reproducibility in weight was obtained between the heating and cooling steps: this indicates that no significant evaporation of material or change in the chemical composition took place. The oxygen content under lower oxygen partial pressures was obtained by monitoring the weight loss under isothermal change of the flowing gas from pure oxygen to mixtures of oxygen in nitrogen [$1\leqslant P(O_2)$ (atm)$\leqslant 1.55\times10^{-4}$]. To obtain the absolute value of the oxygen content, the sample was annealed in oxygen at 550 °C and then reduced in the thermobalance at 550 °C in flowing Ar/H_2 (7% H_2) at the same temperature, which has been selected in order to avoid Bi_2O_3 evaporation and to allow complete reduction.

Electron microprobe analysis was carried out with a JEOL JXA-840A, equipped with three dispersive wavelength spectrometers. The measurements were made with a beam current of 20 nA and a spot of 5 μm^2. Materials were found to have high phase purity ($>99\%$) and homogeneous cation composition: according to the analysis, the phase chemical formula can be written as $Bi_{2.15}Sr_{1.48}Ca_{1.37}Cu_2O_{8.075+\delta}$ which nicely corresponds to the nominal starting composition.

Cu-L_{III} edge x-ray absorption measurements were performed at room- and liquid-nitrogen temperature by using synchrotron radiation from the Synchrotron Radiation Source at the Daresbury Laboratory (Daresbury, U.K.). The samples were thoroughly mixed with a roughly equal amount of graphite (Ventron, 99.5%) in an agate mortar, and then pressed into pellets. The pellets were fixed to stainless-steel sample holders by means of a conductive bi-adhesive tape and then immediately introduced into the experimental chamber at the station 3.4, and pumped down. The spectra were collected in total electron yield mode using a ring current varying from 250 to 200 mA. The thickness of the probed layer can be estimated to be $\cong$200 Å. A double crystal Be($10\underline{1}0$) monochromator was employed. This gives an energy resolution of $\cong$400 meV. To obtain a better signal-to-noise ratio, two different scans, taken in different regions of each samples, have been averaged. The scan to scan reproducibility was shown to be very good ($>99\%$). The spectra were analyzed after (a) subtracting the smooth pre-edge background, fitted with a straight line; (b) calibrating the energy to the CuO Cu-L_{III} peak at 931.2 eV.[16] Each absorption line has been fitted employing a pseudo-Voigt, in order to account for both intrinsic and experimental broadening, showing Lorentzian and Gaussian shape, respectively. The fit has been performed using a MINUIT routine, fitting parameters being energy position, area, width, and Lorentzian/Gaussian character; see Ref. 17 for further details.

In Fig. 1 the oxygen content of the material is reported as a function of temperature and oxygen partial pressure. Data of this figure are in nice agreement with what is reported in the literature[18,19] when the different cation composition of the present samples is taken into account. Figure 2 shows a typical Cu-L_{III} spectrum after background subtraction as described in the experimental section. Near the absorption edge two main lines are apparent. The line at 930.6 eV is unanimously assigned[20] to the $|3d^9\rangle\rightarrow|\underline{2p}_{3/2}3d^{10}\rangle$ transition, i.e., to formally Cu(II) states, the line at 932.2 eV to the $|3d^9\underline{L}\rangle\rightarrow|\underline{2p}_{3/2}3d^{10}\underline{L}\rangle$ transition, i.e., to Cu(III) states. Although a full theoretical approach to this matter is still lacking, several experimental evidences (Refs. 21–23, and references therein) allow us to state that the relative intensity of the two resonance lines reflects the relative density of the corresponding initial states. In short, the actual density of doping holes can be estimated on the basis of the resonance areas; i.e., $[h^{\cdot}]=I_{Cu(III)}/[I_{Cu(III)}+I_{Cu(II)}]$. This ratio should be corrected taking into account the anisotropic distribution of holes. Powder spectra must correspond to single-crystal spectra, with the a,b plane set at 35° with respect to the electric field (a magic angle). This has been verified by comparing Cu-L_{III} spectra of Bi-2212 powders and thin films. Accordingly, a normalization factor equal to 1/0.85 has to be applied to the above formula, in agreement with the doping hole x^2-y^2 symmetry.[21,24] The main source of error is here

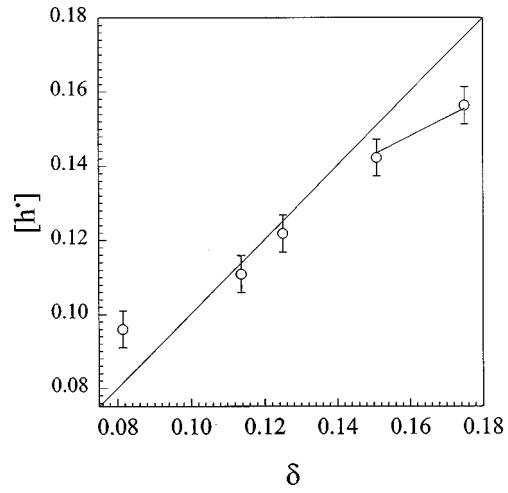

FIG. 3. Doping hole density in $Bi_{2.15}Sr_{1.48}Ca_{1.37}Cu_2O_{8.075+\delta}$. The diagonal line in this plot corresponds to the formation of two holes per copper atom per extra oxygen atom. The small segment joining the last two points corresponds to the formation of one hole per copper atom per extra oxygen atom.

clearly associated with the background subtraction procedure. Errors are likely to equally affect all data, since a systematic procedure has been used: after making use of different choices in background subtraction and with the help of previous experience,[17] the error in the doping hole density can be estimated to be lower than 5%, as is shown by the error bars in Fig. 3.

Actually, further spectral weight can be seen at lower energy (around 928 eV) in Fig. 2. Possibly, it is an experimental artifact or is in some way related to the procedure of data analysis, but we are better inclined to argue that it is a still unexplained real feature of the Cu-L_{III} spectra of cuprate materials. This feature is indeed frequently reported in the literature,[13,21–25] and has been found by our group also on $BaCuO_2$ samples;[17] no significant correlation with oxygen content was found in both cases: indeed, a quite significant correlation is found between the intensity of this feature and the time samples spend in the high-vacuum chamber. For this reason, this feature is tentatively attributed to surface Cu states. It should be noted that this feature is of almost no importance on the final results (i.e., the hole density), its effect being well within the experimental error. The doping hole density as seen by XAS is plotted as a function of the oxygen content in Fig. 3. In this figure, δ values are obtained by subtracting from the overall oxygen content of each sample a reference value of 8.075 needed for the electrical neutrality of the formula. Figure 3 therefore depicts the hole injection sequence induced by oxygen doping in the BSCCO-2212 materials. Three different doping regimes are clearly apparent:

(1) At low oxygen content ($\delta<0.10$) the doping hole density is higher than what is predictable on the basis of δ only. As previously mentioned, this effect has already been described in the literature[13,14] and has been ascribed to the presence near the Fermi level of a band with Bi-O antibonding character, which acts as a source of holes. In chemical terms this can be described by a redox reaction like

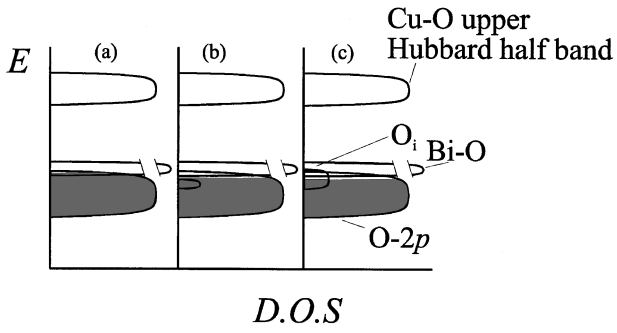

FIG. 4. Band-structure model for $Bi_{2.15}Sr_{1.48}Ca_{1.37}Cu_2O_{8.075+\delta}$. Panels in this figure roughly correspond to (a) $\delta\cong 0$, (b) $\delta\cong 0.12$, and (c) $\delta\cong 0.17$.

$$Bi^{3+}+Cu^{2+}\rightleftarrows Bi^{2+}+Cu^{3+}.$$

(2) At intermediate oxygen content ($0.10<\delta<0.14$) the doping hole density is nearly entirely produced by the oxygen excess only.

(3) The injection of further oxygen atoms ($\delta>0.14$) has a lower effect on the overall hole density. Although this seems to be a fully reasonable result, to the present authors' knowledge it has not yet been described in the literature.

The above results can be interpreted in terms of a simple band-structure model, as drawn in Fig. 4. It is well known that in the Bi-2212 materials the band gap is of a charge transfer nature. In order of increasing energy, near the Fermi level one expects: (i) a filled band mainly O $2p$ in character; (ii) a nearly empty Bi-O antibonding band: superposition (and likely hybridization) of these two bands is responsible for the creation of the extra holes at low δ values; (iii) an empty Cu-O (mainly Cu $3d$ in character) Hubbard half band. Panels in Fig. 4 roughly correspond to the following:

(a) $\delta\cong 0$: No extra oxygen levels are present and the doping hole density is completely determined by the Bi-O antibonding band.

(b) $\delta\cong 0.12$: The injection of extra oxygen atoms creates extra levels, which are expected to live in energy near the O $2p$ band. If all the extra oxygen levels lie under the Fermi level, each extra oxygen atom contributes for two holes to the doping hole density; this lowers the Fermi level under the edge of the Bi-O antibonding band, so that its contribution becomes negligible. Oxygen intercalation in the Bi-2212 material has been reported to increase the formal oxidation state of bismuth to nearly 3 in highly oxygenated samples.[13]

(c) $\delta\cong 0.17$: Further extra oxygen atoms occupy sites with increased energy (this could be reasonably attributed to a Madelung-like potential), and some of the extra oxygen levels lie above the Fermi level. When the Fermi level roughly crosses these levels, each extra oxygen atom contributes one hole to the overall doping hole density.

This work has been partially supported by the Ministero dell'Università e della Ricerca Scientifica e Tecnologica of the Italian Government (MURST-40%). Thanks are given to the Daresbury Laboratory for the provision of the beamtime, and to the Daresbury staff, particularly to Andy Smith, for help during the experiment. Further thanks are due to Pia Riccardi, of the Centro Grandi Strumenti dell'Università di Pavia, for the EMPA.

[1] M. Qvarford, N. L. Saini, J. N. Andersen, R. Nyholm, E. Lundgren, I. Lindau, L. Leonnyuk, S. Soderholm, and S. A. Flodstrom, Physica C **214**, 199 (1993).
[2] K. B. Garg, N. L. Saini, N. Merrien, F. Studer, S. Durkcok, and G. Tourillion, Solid State Commun. **85**, 447 (1993).
[3] A. Bianconi, S. Della Longa, C. Li, M. Pompa, A. Congiu-Castellano, D. Udron, A. M. Flank, and P. Lagarde, Phys. Rev. B **44**, 10 126 (1991).
[4] N. Nücker, J. Fink, J. Fuggle, P. J. Durham, and W. M. Temmermann, Phys. Rev. B **37**, 5158 (1988).
[5] C. F. J. Flipse, G. van der Laan, B. T. Thole, and S. Myra, Z. Phys. B **90**, 89 (1993).
[6] M. Abbate, M. Sacchi, J. J. Wnuk, L. W. M. Schreurs, Y. S. Wang, R. Lof, and J. C. Fuggle, Phys. Rev. B **42**, 7914 (1990).
[7] T. Suzuki, T. Takahashi, T. Kusunoki, T. Morikawa, S. Sato, H. Katayama-Yoshida, A. Yamanaka, F. Minami, and S. Takekawa, Phys. Rev. B **44**, 5381 (1991).
[8] F. J. Himpsel, G. V. Chandrashekhar, A. B. McLean, and M. Shafer, Phys. Rev. B **38**, 11 946 (1988).
[9] M. Matsuyama, T. Takahashi, H. Katayama-Yoshida, T. Kashiwakura, Y. Okabe, S. Sato, N. Kosugi, A. Yagishita, K. Tanaka, H. Fujimoto, and H. Inokuchi, Physica C **160**, 567 (1989).
[10] M. Faiz, J. Jennings, J. C. Campuzano, E. E. Alp, J. M. Yao, D. K. Saldin, and Jaejun Yu, Phys. Rev. B **50**, 6370 (1994).
[11] N. L. Saini, D. S.-L. Law, P. Pudney, K. B. Garg, A. A. Menovsky, and J. J. M. Franse, Phys. Rev. B **52**, 6219 (1995).
[12] N. L. Saini, D. S.-L. Law, P. Pudney, P. Srivastava, A. A. Menovsky, J. J. M. Franse, H. Ohkubo, M. Akinaga, F. Studer, and K. B. Garg, Physica C **251**, 7 (1995).
[13] A. Q. Pham, F. Studer, A. Maignan, C. Michel, and B. Raveau, Phys. Rev. B **48**, 1249 (1993).
[14] A. Q. Pham, H. Hervieu, A. Maignan, C. Michel, J. Provost, and B. Raveau, Physica C **194**, 243 (1992).
[15] G. Flor, P. Ghigna, U. Anselmi-Tamburini, and G. Spinolo, J. Solid State Chem. **116**, 314 (1995).
[16] G. van der Laan, R. A. D. Pattrick, C. M. B. Henderson, and D. J. Vaughan, J. Phys. Chem. Solids **53**, 1185 (1992).
[17] M. Morgante, P. Ghigna, and G. Spinolo (unpublished).
[18] P. Krisnaraj, M. Lelovic, N. G. Eror, and U. Balachandran, Physica C **246**, 271 (1995).
[19] Y. Idemoto, S. Fujiwara, and K. Fueki, Physica C **176**, 325 (1991).
[20] A. Bianconi, A. Congiu-Castellano, M. De Santis, P. Rudolf, P. Lagarde, and A. M. Flank, Solid State Commun. **63**, 1009 (1987).
[21] F. Studer, in *X-Ray Absorption in Bulk and Surfaces*, edited by K. Garg, E. A. Stern, and D. Norman (World Scientific, Singapore, 1994).
[22] F. Studer, C. Gasser, L. Coudrier, H. Murray, M. Pompa, A. M. Flank, and P. Lagarde, Physica B **208-209**, 521 (1995).
[23] J. Fink, N. Nücker, E. Pellegrin, H. Römberg, M. Alexander, M. Knupfer, J. Electron Spectrosc. Relat. Phenom. **66**, 395 (1995).
[24] N. Merrien, F. Studer, G. Poullain, C. Michel, A. M. Flank, P. Lagarde, and A. Fontaine, J. Solid State Chem. **105**, 112 (1993).
[25] N. Merrien, L. Coudrier, C. Martin, A. Maignan, and F. Studer, Phys. Rev. B **49**, 9906 (1994).